Engineering Escherichia coli for methanol conversion

J. E. Muller, F. Meyer, B. Litsanov, P. Kiefer, E. Potthoff, Stephanie Heux, W. J. Quax, V. F. Wendisch, T. Brautaset, Jean-Charles Portais, et al.

▶ **To cite this version:**

J. E. Muller, F. Meyer, B. Litsanov, P. Kiefer, E. Potthoff, et al.. Engineering Escherichia coli for methanol conversion. Metabolic Engineering, 2015, 28, pp.190-201. 10.1016/j.ymben.2014.12.008 . hal-01269203

HAL Id: hal-01269203
https://hal.science/hal-01269203

Submitted on 13 Dec 2023

HAL is a multi-disciplinary open access archive for the deposit and dissemination of scientific research documents, whether they are published or not. The documents may come from teaching and research institutions in France or abroad, or from public or private research centers.

L'archive ouverte pluridisciplinaire **HAL**, est destinée au dépôt et à la diffusion de documents scientifiques de niveau recherche, publiés ou non, émanant des établissements d'enseignement et de recherche français ou étrangers, des laboratoires publics ou privés.

Engineering *Escherichia coli* for methanol conversion

Jonas E.N. Müller, Fabian Meyer, Boris Litsanov, Patrick Kiefer, Eva Potthoff, Stéphanie Heux, Wim J. Quax, Volker F. Wendisch, Trygve Brautaset ,Jean-Charles Portais , Julia A. Vorholt.

Abstract

Methylotrophic bacteria utilize methanol and other reduced one-carbon compounds as their sole source of carbon and energy. For this purpose, these bacteria evolved a number of specialized enzymes and pathways. Here, we used a synthetic biology approach to select and introduce a set of "methylotrophy genes" into *Escherichia coli* based on *in silico* considerations and flux balance analysis to enable methanol dissimilation and assimilation. We determined that the most promising approach allowing the utilization of methanol was the implementation of NAD-dependent methanol dehydrogenase and the establishment of the ribulose monophosphate cycle by expressing the genes for hexulose-6-phosphate synthase (Hps) and 6-phospho-3-hexuloisomerase (Phi). To test for the best-performing enzymes in the heterologous host, a number of enzyme candidates from different donor organisms were selected and systematically analyzed for their *in vitro* and *in vivo* activities in *E. coli*. Among these, Mdh2, Hps and Phi originating from *Bacillus methanolicus* were found to be the most effective. Labeling experiments using ^{13}C methanol with *E. coli* producing these enzymes showed up to 40% incorporation of methanol into central metabolites. The presence of the endogenous glutathione-dependent formaldehyde oxidation pathway of *E. coli* did not adversely affect the methanol conversion rate. Taken together, the results of this study represent a major advancement towards establishing synthetic methylotrophs by gene transfer.

1. Introduction

Methylotrophy represents the ability of microorganisms to utilize reduced one-carbon (C_1) compounds such as methanol or methane as their sole source of carbon and energy. Substantial knowledge in the field has been generated in the past 50 years in particular regarding the occurrence of this trait in microorganisms as well as the set of enzymes and pathways required for methylotrophic growth. Methanol is a non-food alternative substrate to sugar for microbial bioprocess with a competitive price and a sustainable supply. In consequence, interest in methylotrophy is fueled by biotechnological interest in converting raw materials alternative to sugars by microbial fermenta- tion. Although methanol was applied for industrial-scale production of single-cell proteins in the 1970s (Maclenna et al., 1973; Solomons, 1983; Westlake, 1986; Windass et al., 1980), in the past decades interest has shifted to transforming methanol into value-added products including bulk chemicals such as biofuels, amino acids and biopolymers (Schrader et al., 2009; Brautaset et al., 2007), and a methanol-based economy as an alternative fuel and feedstock concept has been proposed (Olah, 2013).

A key question to understanding methylotrophy is how methylo- trophic organisms generate energy and how they convert C_1 substrates such as methanol into carbon compounds with carbon-carbon bonds (carbon fixation and biomass formation). Research efforts with different model species have revealed that methylotrophy consists of a set of functional modules that are ultimately linked to central metabolism and genomes from well-studied model methylotrophs have been determined (Heggeset et al., 2012; Irla et al., 2014; Marx et al., 2012; Vuilleumier et al., 2009). In all methylotrophs, methanol metabolisation is initiated by its oxidation to formaldehyde either by a periplasmic

pyrroloquinoline quinone (PQQ)-containing methanol dehydrogenase in Proteobacteria or an NAD-linked cytoplasmic enzyme in Gram- positives. Because formaldehyde represents an essential but cell-toxic intermediate, its conversion must be efficient. On the one hand, formaldehyde is converted for energy generation *via* non-orthologous pathways (*i.e.*, the ribulose monophosphate (RuMP) pathway, the tetrahydromethanopterin-linked pathway, the glutathione-linked path- way). On the other hand, C_1 assimilation for biomass formation occurs with or without net CO_2 fixation (RuMP cycle, serine cycle, Calvin cycle) (Anthony, 1982; Chistoserdova, 2011; Chistoserdova and Lidstrom, 2013; Vorholt, 2002).

Although it will remain crucial to continue efforts to better understand methylotrophy in natural methylotrophs by using them as the object of interest, we here launch a parallel strategy using synthetic biology concepts related to metabolic engineering with the long term goal of converting non-methylotrophs into methylotrophs. This approach aims at (i) increasing our funda- mental understanding of the process, and (ii) providing access to methanol as a raw material using established platform organisms for methanol conversion into value-added products. The value of applying concepts of design strategies has been noted and criti- cally reviewed (*e.g.*, (Way et al., 2014)) and great progress has been made in providing new standardized working tools and success- fully engineering bacterial metabolism for the production of chemicals. Success in implementing new pathways to "drain" intermediates of central metabolism has been reported for the synthesis of value-added products such as artemisinin and bio- fuels (Kung et al., 2012; Ro et al., 2008). Such product formation had been achieved from carbohydrates (*e.g.* pentoses and glycerol), but hitherto not from C_1 substrates.

Implementing new pathways for carbon influx from a C_1 com- pound represents a difficult task because of the challenging con- densation of C_1 compounds to central metabolites. So far, attempts have been initiated to introduce carbon fixation pathways, and in one study all genes for enzymes for the 3-hydroxypropionate bicycle have been expressed (Mattozzi et al., 2013); however, to our knowledge, no autotrophic pathway has yet been successfully introduced that sustains biomass formation. Additionally, a synthetic CO_2-fixing photorespiratory bypass has been implemented recently (Shih et al., 2014). The aim of generating a synthetic methylotroph represents a particular challenge because both energy demands and biomass requirements must be met by a C_1 source. Moreover, as mentioned above, methylotrophy involves a toxic intermediate and thus any imbalance in metabolism might have fatal consequences.

Here, we use the model bacterium *Escherichia coli* to imple- ment enzymes and pathways for methanol conversion. This choice is justified by the extensive knowledge about its metabolism including a stoichiometric metabolic model (Feist et al., 2007) and the biotechnological interest in the bacterium. Our strategy involves *in silico* modeling and rational criteria for enzyme selec- tion followed by expression of the genes from various donor organisms for empirical testing of their suitability in cell extracts and *in vivo*. We demonstrate that pathways can be successfully established as evidenced by multiple labeled sugar intermediates up to fully labeled hexoses from methanol (C_1).

2. Material and methods

2.1. In silico modeling

For *in silico* modeling approaches the Optflux software (Rocha et al., 2010) version 3.0.7 was used. For modeling we used an *E. coli* model based on (Feist et al., 2007) and added reactions of an NAD- dependent Mdh, a PQQ-dependent Mdh and its associated cyto- chrome *c* oxidase, Hps, Phi, serine glyoxylate aminotransferase, malate thiokinase and malyl-CoA lyase. Furthermore, a reaction was added allowing the creation of methylene-THF from formalde- hyde. During project creation all external metabolites were removed. As biomass reaction R_Ec_biomass_iAF1260_core_59p81M was set.

2.2. Plasmid construction

Oligonucleotides used for construction were obtained from Microsynth (Switzerland) and are also listed in Supplementary Table 1. The plasmids constructed and used in this study are listed in Supplementary Table 2. DNA manipulations were performed using standard protocols (Green et al., 2012). Genes for methanol dehydrogenases and *act* from *Bacillus methanolicus* MGA3 and *B. methanolicus* PB1 were amplified from pET21a plasmids (Krog et al., 2013); other genes for alcohol dehydrogenases, hexulose-6- phosphate synthases and phospho-hexuloisomerases genes used in this study were amplified from genomic DNA. The artificial fusion of Hps and Phi and creation of Mdh activation mutant enzymes was achieved by overlapping PCR. NADP-sensitive Mdh mutant enzymes were constructed following the quick change protocol (Cormack and Castano, 2002). All PCR reactions were performed using Phusion polymerase (Finnzymes), and restriction enzymes were purchased from Fermentas. All constructs were verified by sequencing (Microsynth, Switzerland).

2.3. Gene expression in E. coli and preparation of cell free extracts

LB or M9 medium (400 mL) was inoculated to an OD600 of 0.1 using an overnight culture grown in the same medium. Cells grew to an OD600 of 0.4–0.6, gene expression was induced with 0.1 mM isopropyl-β-D-thiogalactopyranoside (IPTG; Biosynth) and the cells were incubated at 37 °C, 150 rpm for five hours. The cultures were harvested by centrifugation (JA-10 rotor, Avanti J-E, Beckman Coulter) for 10 min at 8000*g* and 4 °C.

Cell free extract was prepared by resuspending cell pellets in 1 mL 50 mM dipotassium phosphate buffer (pH 7.4) supplemented with complete protease inhibitor cocktail tablets (cOmplete, EDTA- free, Roche Applied Science). The cells were disrupted by passing the cell suspension three times through a French pressure cell press (SLM instruments, Thermo Fisher Scientific) at 1000 Psi. Cell debris and membrane fractions were removed by ultracentrifuga- tion (140,000*g* for 60 min at 4 °C). The resulting supernatant was used in enzyme assays.

2.4. Enzyme assays using cell free extracts

Assay of NAD-dependent methanol dehydrogenase activity in cell free extracts. The assay was performed in a total volume of 1 mL in pre-heated (37 °C) 50 mM K_2HPO_4 buffer supplemented with 5 mM $MgSO_4$. The standard assay contained 500 mM NAD^+ (Sigma-Aldrich) and 5–10 mL cell free extract corresponding to 150–300 mg total protein. The reaction was started by addition of 1 M methanol. The production of NADH was continuously measured at 340 nm at 37 °C with a Cary 50 Bio UV–visible spectrophotometer (Varian, Steinhau- sen, Switzerland). Activity was calculated from maximal slopes using the law of Lambert–Beer (ε_{NADH} = 6220 M^{-1} cm^{-1}). One unit (U) was defined as the amount of enzyme that is required to process 1 mmol of substrate per minute. If specific units (U/mg protein) are calcu- lated, the total protein concentration of the lysate was used. Protein concentrations were measured using the Pierce BCA protein assay kit (Thermo Fisher Scientific) with bovine serum albumin (BSA) (Sigma- Aldrich, Buchs, Switzerland) as a standard. All measurements were performed at least in duplicates.

Hexulose-6-phosphate synthase activity assay. The activity of 3-hexulose-6-phosphate synthase (Hps) was determined in a discon- tinuous assay based on the formation of 3-hexulose 6-phosphate from

formaldehyde and ribulose 5-phosphate (Quayle, 1982). The Hps assay contained the following final concentrations: 50 mM potassium phosphate buffer pH 7.4, 5 mM $MgCl_2$, 5 mM formaldehyde, 5 mM ribose 5-phopshate, and 2 U of phosphoriboisomerase (Sigma-Aldrich, Buchs, Switzerland). The reaction mixture was incubated at 37 °C for 15 min and was started by the addition of 10 ml cell free extract. Samples (100 mL) were taken every 60 s and mixed with 100 ml 0.1 M HCl solution to stop any enzymatic activity. The samples were stored on ice until the end of the experiment. Finally, protein precipitates were pelleted by centrifugation at 16,000*g* and 4 °C for 10 min, and the formaldehyde concentration was determined (Nash, 1953).

3-Phospho-6-hexuloisomerase activity assay. The activity of 6-phospho-3-hexuloisomerase (Phi) was determined in a direction that opposed the physiological reaction by measuring the forma- tion of formaldehyde from fructose 6-phosphate with a coupled discontinuous enzyme assay with functional Hps (demonstrated with the corresponding assay). The Phi assay contained a final concentration of 50 mM potassium phosphate buffer at pH 7.4, 5 mM $MgCl_2$, and 50 mM fructose 6-phosphate (Sigma-Aldrich, Buchs, Switzerland). The reaction was incubated at 37 °C for 10 min and was started by the addition of 10 ml cell free extract. Sampling and assay readouts were performed as described above for the Hps assay.

2.5. Enzyme activities in vivo by formaldehyde production/ consumption

Mdh assay. Cells were grown overnight in M9 medium supple- mented with glucose (0.4%) and the respective antibiotics. The next morning, 50 mL of M9 medium supplemented with antibiotics and 0.1 mM IPTG was inoculated to an OD600 of 1. Cells were grown at 37 °C with vigorous shaking until stationary phase was reached (checked by OD600 measurements). Then an amount of cells corre- sponding to an OD600 of 1 in a volume of 50 mL was pelleted by centrifugation at 8000 rpm for 10 min at room temperature. The cells were washed twice in water and pelleted as described above between the steps. Finally, the pellet was re-suspended in 50 mL of standard M9 medium without glucose and the actual OD600 was measured. The experiments were started by addition of 2 mL 10% methanol resulting in a final concentration of 1 M. Directly after the addition of methanol, a starting sample of 600 mL was taken and from there on samples were taken every 5 min. The samples were centrifuged for 5 min at 11,000*g* at 4 °C to remove the cells. A total of 500 mL of the supernatant was mixed with Nash reagent and the formaldehyde concentration was determined according to Nash (1953). Throughout the experiment, cultures were kept at 37 °C in a shaking water bath. One unit (U) was defined as 1 mmol formaldehyde produced per 1 min. For calculating specific units (U/mg protein), the protein concentration was estimated based on the OD600 of the culture and the assumption that 1 L culture with an OD600 of 1 contains 0.250 g of biomass of which half is assumed to be protein.

Hps Phi assay. Preparation of the cells and sampling was performed as described above with the difference that the reaction was started by adding 0.5 mM formaldehyde instead of methanol. Formaldehyde concentration measurements and activity calcula- tions were performed as described above. When ribose was used as a carbon source the cells were cultivated in and tested in M9 medium containing 10 mM ribose instead of glucose.

2.6. Dynamic labeling incorporation

Precultures of strains to be tested were directly inoculated from glycerol stocks in 5 mL M9 medium containing 20 mM ribose and 0.2% casamino acids to allow efficient protein production. Medium was supplemented with antibiotics, as appropriate, and 0.1 mM isopropyl-β-D-thiogalatopyranosid (IPTG). Cultures were grown over night at 37 °C and 150 rpm in culture tubes. The next morning precultures were used to inoculate 20 mL M9 medium with reduced phosphate concentration (2 mM) to an OD600 of 0.1–0.2. The medium again contained 20 mM ribose, antibiotics and 0.1 mM IPTG but no casamino acids. Strains were grown at 37 °C and 150 rpm for app. 6 h in 100 mL shake flasks with baffles. Growth was followed by measuring OD600. For the actual experiment, an amount of cells equal to OD600 of 0.5 in a volume of 10 mL was pelleted (5 min, 10,000 g, RT). The cells were washed with 20 mL sterile deionized water and pelleted again (5 min, 10,000 g, RT). Finally, cells were resuspended in 10 mL M9 medium with reduced phosphate concentration without any carbon source but required antibiotics and 0.1 mM IPTG and transferred into pre-warmed shaking flasks with baffles. Before the experiment was started OD600 was measured. Throughout the experiment flasks were shaken at constant speed in a water bath at 37 °C. Before starting the experiment by addition of 400 μL ^{13}C labeled methanol (Cambridge Isotope Laboratories) which correspond to a final concentration of 1 M a sample was taken. After addition of labeled substrate, samples were taken 3 min, 6 min and 10 min after the start. For each sample 1 mL culture was transferred onto a polyethersulfone (PESU) 0.2 μm filter (Sartorius Stedim) pre-washed with an excess amount of 50 °C hot water. By applying vacuum, the medium was removed and the cells were washed with 1 mL 20 °C warm MilliQ water. The filter with cells was transferred into 1.5 mL–20 °C cold quenching solution and kept on ice for app. 10 min with short intervals of sonification. The filters were removed, samples were frozen in liquid nitrogen and lyophilized overnight. Sampled biomass amount was app. 125 μg cell dry weight (CDW) assuming OD CDW correlation factor of 0.25 mg/mL. Lyophi- lized samples were resuspended in MilliQ to give a final biomass concentration of 1 μg/μL. The resuspended samples were centrifuged at 20,000*g* for 10 min at 4 °C and 20 μL. Prior to LC–MS analyses, samples were mixed with 80 μL ammonium acetate buffer pH 8.0 containing 1.6 mM of ion pairing reagent tributylamine.

Nanoscale ion-pair reversed phase HPLC–MS. Metabolome analysis of the prepared ^{13}C labeling experiment samples was carried out by using nanoscale ion-pair reversed-phase high performance liquid chromatography (nano-IP-RP-HPLC) with a split-free nanoLC Ultra system (Eksigent, Dublin, CA) hyphenated to an LTQ-Orbitrap mass spectrometer (ThermoFisher Scientific, San Jose, CA) by nanoelectros- pray ionization as described previously with slight modification (Kiefer et al., 2011) as follows. Separation of the metabolites was performed on a C18 column (Dr. Maisch HPLC Markensäule, Reprosil-Gold 120, 100 mm x 0.1 mm, Morvay Analytik GmbH) as stationary phase with a tributylamine (TBA) solution as the ion-pairing reagent and methanol (solvent B) as eluent. The TBA solution (solvent A) was obtained by dissolving 1.7 mM TBA in 1.5 mM acetic acid and adjusting the pH to 9.0 with 6 M ammonium hydroxide. Solvent B (methanol) was varied according to the gradient; 0 min, 3%; 30 min, 90%; 35 min, 90%; 36 min, 3%; 45 min, 3% with a flow rate of 400 nL/min. The injection volume was 1 μL. Mass acquisition was done in the negative Fourier transform mass spectrometry mode with AGC target setting of 500,000 at unit resolution of 60,000 (at m/z 400) applying an ion spray voltage of 1.9 kV. The capillary temperature was 150 °C and the capillary voltage was set at − 10 V. Acquisition was performed in scan mode for the mass ranges 150m/zr850. Obtained MS-data were analyzed using eMZed 1.3 (Kiefer et al., 2013).

3. Theory

3.1. Engineering strategy

Establishing heterologous pathways is often challenging and sev- eral aspects, *e.g.*, number of required proteins, their dependency on co- factors and toxicity of produced metabolites, have to be taken into account. To enable *E. coli* to utilize methanol, the C_1 substrate must be

converted by unique enzymes and subsequently connected *via* inter- mediates to central metabolism and thus converted into metabolites naturally used by *E. coli.* As outlined above, in all known aerobic methylotrophs, methanol is first converted to formaldehyde catalyzed by a methanol dehydrogenase (Mdh). Because *E. coli* is a Gram- negative bacterium, a PQQ-dependent periplasmic Mdh used by Gram-negative methylotrophs (Anthony and Williams, 2003) such as the best characterized enzyme from *Methylobacterium extorquens* AM1 could be an obvious choice. The enzyme is highly efficient towards methanol, however, at least 11 gene products are necessary for its functional assembly (Chistoserdova et al., 2003). Although *E. coli* possesses a PQQ-dependent glucose dehydrogenase, this bacterium is not able to synthesize this cofactor (Anthony, 2004) making it necessary to also insert the PQQ biosynthetic pathway (Wagh et al., 2014; Yang et al., 2010) or alternatively the cells will remain dependent on PQQ addition to the growth medium. The electron acceptor of this Mdh is cytochrome c_L, which is subsequently oxidized by a terminal cytochrome c oxidase (Anthony, 2004), which are both absent in

E. coli. Taken together, functional production of a PQQ-dependent Mdh in *E. coli* includes several major experimental hurdles bearing an elevated risk regarding successful implementation. In contrast, the Mdh of the Gram-positive *B. methanolicus* requires only one gene for functional production (Krog et al., 2013; Ochsner et al., 2014). The enzyme is NAD-dependent, allowing the direct use of the electron acceptor in *E. coli* and rendering NAD-dependent Mdh an obvious target of choice for implementation in *E. coli* and for oxidation of methanol to formaldehyde.

Realizing the next step of formaldehyde oxidation in *E. coli* might not necessarily depend on the introduction of a hetero- logous pathway. As formaldehyde is a toxic compound formed in classical metabolism at low concentrations as a result of demethy- lation reactions (Case and Benevenga, 1977), *E. coli* like other organisms possesses a formaldehyde detoxification pathway linked to glutathione (GSH) (Gonzalez et al., 2006; Gutheil et al., 1992) that involves a glutathione (GSH)-dependent formaldehyde dehydrogenase encoded by the gene *frmA* (Duine, 1999). Notably, this detoxification pathway is similar to the linear GSH-dependent formaldehyde oxidation pathways found in some methylotrophic organisms (Gonzalez et al., 2006; Gutheil et al., 1992). Conse- quently, the introduction of such a linear pathway might not be essential for formaldehyde oxidation in *E. coli*.

Regarding assimilation of formaldehyde into biomass, the three major pathways in natural methylotrophs have been noted above, and within the scope of this work we considered the RuMP cycle and the serine cycle of "true" methylotrophs which are able to assimilate formaldehyde for biomass formation. Different variants of both path- ways are known to exist in nature (Anthony, 1982). The RuMP cycle is classically divided into fixation, cleavage and rearrangement phases. The fixation phase is similar in all organisms and employs the enzymes hexulose-6-phosphate synthase (Hps) and 6-phospho-3-hexuloisom- erase (Phi) (Fig. 1), whereas for the cleavage and rearrangement phases variations exist. During the cleavage phase, either a fructose-bisphosphate aldolase (FBPase variant) or a keto-hydroxyglutarate aldolase (KDPG aldolase variant) is used to decompose C6 metabolites to glyceraldehyde phosphate and dihydroxyacetone phosphate or glyceraldehyde and pyruvate. Regeneration of the initially required ribulose-5-phosphate takes place either *via* a sequence of reactions involving transaldolase (the transaldolase variant) or sedoheptulose bisphosphatase (the sedoheptulose bisphosphatase variant). Closer inspection of all possible variants revealed that with the exception of Hps and Phi enzymes, most variants are naturally present in *E. coli* because they are needed for glycolysis (FBPase), the Entner-Doudoroff pathway (KDPG aldolase) or the pentose phosphate pathway (transal- dolase). Thus, theoretically only two heterologous proteins need to be produced to establish a functional RuMP cycle in *E. coli*.

In contrast to the RuMP cycle, the serine cycle does not assimilate formaldehyde directly; instead formaldehyde binds to tetrahydrofo- late (THF) in the form of methylene-THF and is added to glycine to form serine. Serine is subsequently transformed in a series of reactions to yield phosphoenol-pyruvate before it is carboxylated by phosphoenolpyruvate carboxylase to form oxaloacetate. Unlike the RuMP cycle, two C_1 units are fixed by the reactions of the serine cycle, first in the form of cofactor-bound formaldehyde and subse- quently as CO_2 during the carboxylation reaction of phosphoenolpyr- uvate carboxylase. The resulting oxaloacetate is converted into malyl- CoA, which is cleaved into two 2-carbon compounds, glyoxylate and acetyl-CoA (Anthony, 1982). Finally, the conversion of glyoxylate into glycine regenerates the acceptor molecules and closes the cycle. To balance the reactions, acetyl-CoA is regenerated to glyoxylate *via* the ethyl-malonyl-CoA pathway (EMCP) in isocitrate lyase (Icl)-negative organisms (EMCP variant) or *via* citrate and isocitrate (glyoxylate shunt) in Icl-positive organisms (ICL variant) (Erb et al., 2007; Peyraud et al., 2009). Depending on the variant, the assimilation of two molecules of formaldehyde and one CO_2 (ICL-variant) or three formaldehydes and three molecules of CO_2 (EMCP variant) leads to the net formation of one or two molecules of 2-phosphoglycerate, respectively. Except for serine glyoxylate aminotransferase, malate thiokinase and malyl-CoA lyase, all enzymes for the cycle are present

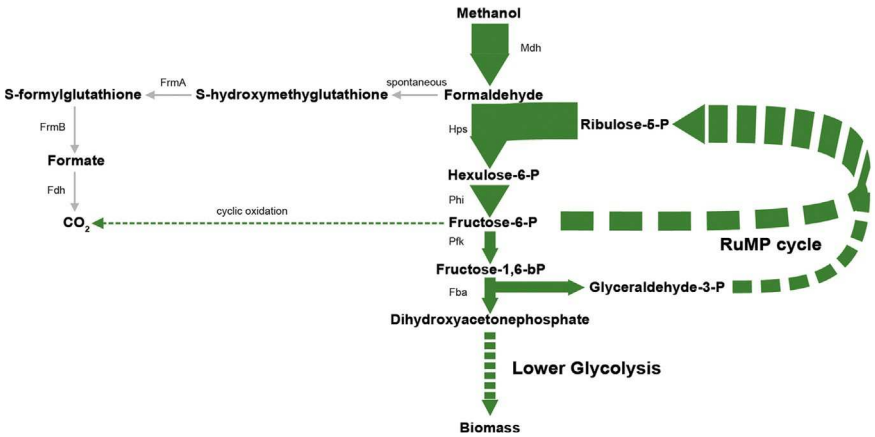

Fig. 1. Scheme of engineered *E. coli* metabolism. Metabolic fluxes in a hypothetical methylotrophic *E. coli* are calculated for growth on methanol based on a genome-scale metabolic model and optimizing biomass yield as objective function. Green arrows indicate flux, and the size of the arrows corresponds to the calculated flux. Influx of methanol was set to 42 mmol/g x h. Mdh, methanol dehydrogenase; Hps, 3-hexulose-6-phosphate synthase; Phi, phosphohexulo-isomerase; Pfk, phosphofructokinase; Fba, fructose bisphosphate aldolase; FrmA, formaldehyde dehydrogenase A; FrmB, S-formylglutathione hydrolase; Fdh, formate dehydrogenase. Broken lines represent multiple reactions. For a more detailed map and calculated fluxes see Supplementary Fig. 1.)

in *E. coli*, and while establishing the EMCP variant for glyoxylate regeneration would require several heterologous enzymes, all enzymes for the ICL variant are present in *E. coli*. Establishing the serine cycle with the ICL variant would require production of three heterologous enzymes; however, it would also involve a potential shortcoming to establish sufficient flux required for the condensation of formaldehyde with THF (Kallen and Jencks, 1966a, 1966b; Kay et al., 1960), and no formaldehyde activating enzyme for this reaction has been identified yet, in contrast to other formaldehyde cofactor condensation reactions (Goenrich et al., 2002; Vorholt et al., 2000). In addition, carbon assimilation *via* the serine cycle involves significant CO_2 fixation reactions (50% in *M. extorquens*, (Peyraud et al., 2009)), in contrast to the RuMP cycle where a single entry point of reduced carbon exists in the form of formaldehyde, and which is thus energetically more favorable (Schrader et al., 2009).

3.2. *In silico validation of the engineering strategy*

To test the preferred choice of enzymes and pathways outlined above, all potential pathways were examined *in silico* for valida- tion purposes. To this end we modified a stoichiometric genome- scale *E. coli* model (Feist et al., 2007) and integrated reactions representing NAD-dependent Mdh, PQQ-dependent Mdh and its associated cytochrome c oxidase, Hps and Phi to establish the RuMP cycle, and finally serine glyoxylate aminotransferase, malate thiokinase and malyl-CoA lyase to establish the serine cycle.

In total, the model contained 1271 gene products and reactions with 1676 metabolites. We used flux balance analysis (FBA) with maximal biomass yield (equals growth rate m) as a constraint and either methanol or glucose as the carbon source. The uptake rate of glucose was set to 7 mmol/(g_{CDW} x h), which corresponds to the glucose uptake rate of *E. coli* in shake flasks (Fischer et al., 2004; Nicolas et al., 2007). For comparison, we adjusted the influx of methanol to equal the amount of carbon that is taken from glucose, and we set the influx of methanol to 42 mmol/(g_{CDW} x h). With glucose as carbon source the predicted maximal growth rate (m) was 0.65 h^{-1}, which was in perfect agreement with the measured m of 0.65 h^{-1} (Nicolas et al., 2007). The integration of several methylo- trophic enzymes allowed the model to find a feasible solution with methanol as a carbon source and a maximal m of 0.88 h^{-1} was predicted, indicating that methanol can principally be metabolized at least as efficiently as glucose. Closer inspection revealed that the model chose the NAD-dependent Mdh over the PQQ-dependent enzyme, and for biomass accumulation, the RuMP cycle rather than the serine cycle was preferred (Fig. 1). This solution was accom- plished by using the introduced enzymes Hps and Phi and the enzymes of the non-oxidative pentose phosphate pathway. All endogenous reactions showed flux in the reverse direction compared to the flux during glucose-based growth (Supplementary Fig. 1). However, because these enzymes are reported to be reversible, the flux direction allowing for growth on methanol should be possible *in vivo* as well. By deletion of Hps and/or Phi, the model could be forced to use the serine cycle; however, this resulted in a lower growth rate, which was also true if utilization of the PQQ-dependent Mdh was enforced.

The model predicted that the citric acid cycle was not closed, which is in line with knowledge available from natural methylo- trophs during growth on methanol (Chistoserdova et al., 2009), and it was only used for cataplerosis in our simulation. Only approximately 5% of the produced formaldehyde was oxidized to CO_2, and to this end, the established dissimilatory RuMP cycle was used while no flux through the endogenous GSH-dependent pathway was predicted. In conclusion, the model supports the idea that introduction of three additional genes might be sufficient to allow biomass formation in *E. coli.*

4. Experimental results

4.1. *Identification, expression and functional testing of C_1-converting enzymes in cell free extracts of E. coli*

The successful implementation of the *in silico*-validated engi- neering strategy for synthetic methylotrophy into *E. coli* requires overcoming several major steps at different complexity levels. The initial step consists of making appropriate choices for the different enzymes and empirically testing them for catalytic activity, first in cell extracts and subsequently *in vivo*. To ensure modular testing of enzyme combinations we chose a cloning strategy using plasmids based on the Standard European Vector Architecture (pSEVA) (Silva-Rocha et al., 2013).

Taking into account the results of the *in silico* modeling and given the biological constraints of PQQ-dependent Mdh, we decided to focus our efforts on an approach involving an NAD-dependent Mdh and establishment of the RuMP cycle by heterologous production of Hps and Phi. Recently, it was discovered that wild-type strains of *B. methanolicus* harbor several genes encoding NAD-dependent Mdhs and that all of them can be functionally produced in *E. coli* (Krog et al., 2013). Previous studies have shown (Arfman et al., 1997, 1991) that the *in vitro* activity of analyzed Mdh is strongly increased in the presence of the activator protein Act. To increase the chances of finding an enzyme capable of efficient methanol oxidation in *E. coli*, we decided to test not only enzymes of *B. methanolicus* but also alcohol dehydrogenases with a potential for methanol oxidation. This strategy to find additional candidate enzymes was also justified by the optimal growth temperature of *B. methanolicus* of 50–55 °C, which is well above the optimal growth temperature of *E. coli* (37 °C). Although we recently validated that *B. methanolicus* is capable of growth on methanol at 37 °C, the growth rate was found to be significantly reduced (0.14 h^{-1} instead of 0.4 h^{-1}) (Müller et al., 2014), and thus enzymes from other organisms might operate with more favorable catalytic efficiency. To identify additional Mdhs for our implementation strategy, we used BLAST searches and identified NAD-dependent alcohol dehydrogenases in *Bacillus coagulans*, *Desul- fotomaculum kuznetsovii*, *Desulfitobacterium hafniense*, *Lysinibacillus fusiformis* and *L. sphaericus*. Purification and characterization of these enzymes led to the finding that all of them are also susceptible to activation by Act *in vitro* (Ochsner et al., 2014). To ensure that all the enzymes are functionally produced in *E. coli* and also active under *E. coli* growth conditions, we tested activity with and without Act in cell free extract at 37 °C (Table 1). The activity in cell extracts was detectable but generally low at this temperature and pH 7.4 (note that these enzymes were generally only characterized under non- physiological pH of 9.5) and ranged from 1.4 mU/mg for Mdh of *B. methanolicus* MGA3 to 5.8 mU/mg for Adh of *B. coagulans* without Act and from 3.8 mU/mg for Adh of *L. fusiformis* to 45 mU/mg for Mdh2 of *B. methanolicus* MGA3 with Act. We tried to boost the activity further by using stronger promoters and increasing gene dosage based on plasmid copy number and simultaneous expression from different plasmids. However, no increase in activity could be observed (data not shown).

Hektor et al. identified a mutation (S97G) in Mdh of *B. methano- licus* strain C1 that increased the activity of the enzyme by mimicking the effect of Act (Hektor et al., 2002). This mutation was introduced into Mdh, Mdh2 and Mdh3 of *B. methanolicus* MGA3 by us previously and studied (Ochsner et al., 2014). Here, we tested all three mutant enzymes for their activity in *E. coli* lysate under *E. coli* physiological conditions. As reported for the purified enzyme, the "activation mutation" increased the activity of Mdh from 1.4 mU/mg to 5.1 mU/mg, however, it attenuated activity of Mdh2 and Mdh3 (Table 1).

We also tested site-directed mutant variants that use $NADP^+$ in addition to NAD^+ as a cofactor (Ochsner et al., 2014) because we speculated that a broadened cofactor specificity might increase the

Table 1
In vitro and *in vivo* activities of different methanol and alcohol dehydrogenases from different organisms in *E. coli* in the presence or absence of Act. *In vitro* activities were measured in cell free extract of *E. coli*, *in vivo* activities were measured in *E. coli* cell suspensions. n.a.: data not available.

Enzyme(s)	*In vitro* activity [mU/mg]	*In vivo* activity [mU/mg]
Mdh *B. methanolicus* MGA3	1.4	1.7
Mdh *B. methanolicus* MGA3þAct	15.5	0.7
Mdh2 *B. methanolicus* MGA3	2.3	30
Mdh2 *B. methanolicus* MGA3þAct	45	21.3
Mdh3 *B. methanolicus* MGA3	1.5	23
Mdh3 *B. methanolicus* MGA3þAct	27.3	n.a
Mdh *B. methanolicus* PB1	2.6	0.7
Mdh *B. methanolicus* PB1þAct	n.a.	n.a.
Mdh1 *B. methanolicus* PB1	10	0
Mdh1 *B. methanolicus* PB1þAct	n.a.	n.a
Mdh2 *B. methanolicus* PB1	3.3	3
Mdh2 *B. methanolicus* PB1þAct	n.a.	n.a.
Adh *L. sphaericus* C3-41	2.9	1
Adh *L. sphaericus* C3-41þ Act	8.4	n.a.
Adh *L. fusiformis* ZC1	3.8	0
Adh *L. fusiformis* ZC1þ Act	3.8	n.a.
Adh *B. coagulans* 36D1	5.8	3
Adh *B. coagulans* 36D1þAct	15.5	n.a.
Adh *D. hafniense* Y51	1.8	7
Adh *D. hafniense* Y51þAct	16.7	n.a.
Adh *D. kuznetsovii*	n.a.	n.a.
Adh *D. kuznetsovii* þ Act	n.a.	n.a.
Mdh *B. methanolicus* MGA3 S97G	5.1	14
Mdh *B. methanolicus* MGA3 S97Gþ Act	21	n.a.
Mdh2 *B. methanolicus* MGA3 S97G	0.8	2.1
Mdh2 *B. methanolicus* MGA3 S97GþAct	0.9	n.a.
Mdh3 *B. methanolicus* MGA3 S97G	0.7	0.7
Mdh3 *B. methanolicus* MGA3 S97GþAct	0.6	n.a.
Mdh *B. methanolicus* MGA3 D38G	6.5	0.3
Mdh *B. methanolicus* MGA3 D38GþAct	n.a.	n.a.
Mdh2 *B. methanolicus* MGA3 D38G	5.9	0.4
Mdh2 *B. methanolicus* MGA3 D38GþAct	n.a.	n.a.

chances for successful application *in vivo*. The mutants of Mdh and Mdh2, which were able to use NADPþ, additionally performed well when tested with NADþ under *E. coli* physiological conditions with an activity of 6.5 mU/mg and 5.7 mU/mg, respectively (Table 1).

To identify Hps and Phi enzymes suitable with respect to their production and activity in *E. coli*, we screened several organisms. In addition to using Hps and Phi of *B. methanolicus* we also tested enzymes from *Methylobacillus flagellatus* KT and *Methylococcus capsulatus* (Bath), which are both Gram-negative methylotrophs employing the RuMP cycle for biomass accumulation (Chistoserdova et al., 2007; Ward et al., 2004). The genome of *M. flagellatus* indicates the presence of two paralogous *hps* genes (Mfla250 and Mfla1654) (Chistoserdova et al., 2007). The primary sequences of the gene products are 35% and 36% identical, respectively, to Hps from *B. methanolicus* MGA3. Mfla1654 is located in an operon with a potential Phi encoding gene, Mfla1653, which encodes a protein 32% identical to Phi of MGA3.

M. capsulatus harbors potential Hps coding genes (MCA3043, MCA3049 and MCA2738), of which the first two are identical copies encoding a protein with 34% similarity to Hps of *B. methanolicus* MGA3 (Ward et al., 2004). *M. capsulatus* encodes a protein that represents an Hps Phi fusion with an N-terminal Hps part with 35% sequence identity and a C-terminal part 40% identical to Phi from *B. methanolicus* MGA3. Interestingly, bifunctional Hps Phi enzymes have already been described for archaea (Orita et al., 2005), and an artificial fusion of Hps and Phi can enhance the overall activity as shown for the Hps Phi pair of *Mycobacterium gastrii* MB19 (Orita et al., 2007). We therefore decided to test the enzyme of *M. capsulatus* and artificially fuse Hps and Phi enzymes of *B. methanolicus* MGA3 and *M. flagellatus* KT, respectively, by overlap PCR to examine whether the fusion also increases activity.

Hps catalyzes the condensation of formaldehyde to ribulose 5-phosphate thereby producing hexulose 6-phosphate (Fig. 1). To test this activity in cell free extracts, formaldehyde degradation was measured using a discontinuous assay. Hps enzymes displayed high activities between 0.7 and 9 U/mg (Table 2). None of the fused Hps Phi derivatives of *B. methanolicus* and *M. capsulatus* showed activity. The fusion of the *M. flagellatus* enzymes led to a four-fold decreased activity (0.7 mU/mg) compared to Hps alone (3.2 U/mg). In consequence, the Hps from *B. methanolicus* was the most active enzyme in this assay (9.0 U/mg). This level of activity is in line with previous kinetic characterizations of this enzyme (Arfman et al., 1990, 1989). Phi converts the Hps product hexulose 6-phosphate into fructose 6-phosphate, which then is further converted in the RuMP cycle (Fig. 1). Due to the instability of hexulose 6-phosphate, Phi activity was measured in the reverse direction. Fructose 6-phosphate was used as a substrate in the production of formaldehyde in a coupled reaction together with Hps. In all lysates with Hps activity, Phi activity was detected, but the overall activities measured were lower (Table 2). The highest activity was observed in cell extracts containing the *B. methanolicus* Phi enzyme.

To benchmark the activities of the heterologously produced enzymes in *E. coli*, we compared the best performing Mdh2 enzymes produced together with Act, Hps and Phi of *B. methanolicus* MGA3 *in vitro* with activities of the respective enzymes in cell free extracts of methanol grown *B. methanolicus* (Müller et al., 2014). Mdh2 activity measured in *E. coli* lysate was 220 mU/mg, similar to the activity determined in *B. methanolicus* (210 mU/mg) when tested under the same conditions (pH 9.5 and 45 °C). Hps and Phi activities in *E. coli* lysate (9.3 U/mg and 0.7 U/mg) reached more than 50% of the activities measured in *B. methanolicus* lysate (17 U/mg and 1.0 U/mg). Taken together, for all heterologous enzyme reactions required, we identified proteins that could be actively produced in *E. coli*. Furthermore, the most active candidates reached activity levels very similar to the ones detected in a natural methylotroph, showing that the protein levels are potentially high enough to allow for sufficient methanol utilization.

4.2. Analysis of C_1-converting enzymes in vivo by measuring formaldehyde formation and fixation

Even more relevant for pathway operation in a heterologous system is the determination of the *in vivo* activity of the different enzymes. To this end, we developed a discontinuous enzyme assay based on the detection of formaldehyde production by cells producing a functional Mdh upon addition of methanol. Because formaldehyde produced by Mdh can freely diffuse through the cell membrane, formaldehyde concentration changes can be directly determined in the medium. In a first step we tested the activity of functionally produced Mdh and Mdh2 from *B. methanolicus* in *E. coli* cell suspensions where we could indeed detect formaldehyde accumulation due to the oxidation of methanol. When using *E. coli* wild-type strain for the assay, an initial phase of formaldehyde accumulation was followed by a decrease in formaldehyde concentration (Fig. 2A). This observation indicated that the endogenous glutathione-dependent formaldehyde detoxification pathway of the host might have been activated. To test this hypothesis and to prevent the induction of formaldehyde detoxification, we used an *E. coli* mutant strain, Δ*frmA*, with a deletion in formaldehyde dehydrogenase (*frmA*) and observed that formaldehyde was indeed only accumulating in the case of *mdh* expression (Fig. 2A). In consequence, all other potential enzymes were tested in a Δ*frmA E. coli* background. Of all the tested Mdh enzymes, Mdh2 of *B. methanolicus* MGA3 showed the highest *in vivo* activity with 30 mU/mg (Table 1). With the exception of Mdh3 from the same organism which showed an activity of 23 mU/mg, the activities of all other tested enzymes were

Table 2
In vivo and *in vitro* activities of Hps and Phi enzymes from different organisms in *E. coli*. *In vitro* activities were measured in cell free extract of *E. coli*, *in vivo* activities were measured in *E. coli* cell suspensions. Wt, *E. coli* wild-type cells; Δ*frmA*, *E. coli* Δ*frmA* cells; n.a., data not available; n.d., activity not detected. Measured enzyme is indicated in bold.

Enzyme	*In vitro* activity [U/mg]	*In vivo* activity [U/mg]
Hps Phi operon *B. methanolicus* MGA3 (Wt)	5.5	0.26
Hps Phi operon *B. methanolicus* MGA3 (Δ*frmA*)	9.3	0.16
Hps Phi fusion *B. methanolicus* MGA3 (Wt)	n.d.	n.a
Hps Phi fusion *B. methanolicus* MGA3 (Δ*frmA*)	n.d.	n.a.
Hps Phi operon *M. flagellatus* KT (Wt)	3.7	0.17
Hps Phi operon *M. flagellatus* KT (Δ*frmA*)	2.3	0.14
Hps Phi fusion *M. flagellatus* KT (Wt)	1.2	0.15
Hps Phi fusion *M. flagellatus* KT (Δ*frmA*)	0.7	0.12
Hps Phi fusion *M. capsulatus* Bath (Wt)	n.d.	n.a.
Hps Phi fusion *M. capsulatus* Bath (Δ*frmA*)	n.d.	n.a.
Hps Phi operon *B. methanolicus* MGA3 (Wt)	0.9	n.a.
Hps Phi operon *B. methanolicus* MGA3 (Δ*frmA*)	0.7	n.a.
Hps Phi operon *M. flagellatus* KT (Wt)	0.3	n.a.
Hps Phi operon *M. flagellatus* KT (Δ*frmA*)	0.4	n.a.
Hps Phi fusion *M. flagellatus* KT (Wt)	0.2	n.a.
Hps Phi fusion *M. flagellatus* KT (Δ*frmA*)	0.1	n.a.

significantly lower. Surprisingly, no difference in enzyme activity was detected when *act* was expressed in conjunction (Table 1, Fig. 2B).

Next, we assayed the *in vivo* activity of the Hps Phi constructs that showed the highest activity *in vitro*. To take into account formaldehyde conversion, which can proceed *via* Hps Phi but also the glutathione-dependent formaldehyde pathway, we used both an *E. coli* wild-type background and Δ*frmA* (Fig. 2C). As already observed in previous experiments (Fig. 2A), formaldehyde degra- dation in wild-type cells by the endogenous glutathione-depe- ndent pathway started with a delay. In contrast, formaldehyde degradation by Hps Phi in Δ*frmA* and wild-type host cells started right after the addition of formaldehyde (Fig. 2C). In a first set of experiments, formaldehyde degradation was analyzed in resting cells in M9 medium without any carbon source. Activities between 10 and 20 mU/mg were detected in this assay (Fig. 2C). This was surprisingly low considering that the Hps activity measured *in vitro* was up to 9 U/mg, which is almost three orders of magnitude higher. In addition to formaldehyde, ribulose 5-phosphate is needed as a substrate during the Hps-catalyzed reaction. We speculated that the availability of C_5 compounds in glucose-grown cells might be too low to allow fast assimilation of formaldehyde, especially because the actual experiment was performed in the absence of any carbon source. To increase the *in vivo* activity, the experiment was repeated with cells grown in ribose as sole carbon source. It turned out that cells growing in ribose and adding ribose during the assay as a carbon source increased the activity observed with the Hps Phi constructs. In all cases approximately 10 times higher activity compared to conditions without any multicarbon source was observed. The *B. methanolicus* Hps Phi showed the highest activity (up to 260 mU/mg) (Table 2). To verify that the observed effect is caused by supplying C_5 precursor molecules and not simply by the availability of a carbon source, the experiment was repeated for Hps of *B. methanolicus* with glucose instead of ribose. The activity measured under these condi- tions was higher than without any carbon source, 51 mU/mg *vs* 20 mU/mg, but three times less compared to the ribose experiment. This observation confirmed that the availability of C_5 precursors is crucial for the rapid assimilation of formaldehyde.

In a subsequent experiment, we tested whether Mdh2, Hps and Phi of *B. methanolicus* MGA3 function together by monitoring if formaldehyde accumulation was lower *in vivo* when all three enzymes were present compared to Mdh2 alone. Because the *in silico* simulations suggested that a linear formaldehyde oxidation pathway is not necessary and formaldehyde conversion by Hps and Phi can principally compete with such a pathway, the *in vivo* activity was also tested in the Δ*frmA* background. If only Mdh2 was produced, formaldehyde accumulated faster and up to a level of approximately 0.12 mM (Fig. 2D). If Hps and Phi were produced together with Mdh2, the maximal level of formaldehyde observed was lowered to 50 mM, suggesting that Mdh2 and Hps/Phi are functionally produced in the same cells and that formaldehyde produced by the former is metabolized by the latter.

4.3. Testing of C_1-converting enzymes in vivo using dynamic ^{13}C labeling

Although *in vitro* and *in vivo* experiments indicated that the enzymes for methanol utilization were functionally produced and capable of methanol metabolism, the effect of integration on the metabolic system of *E. coli* remained to be investigated. To improve our understanding on how the metabolism of *E. coli* is changed in the presence of a methanol-oxidizing enzyme together with Hps and Phi and to examine to what extent methanol assimilation is allowed in concert with *E. coli*'s endogenous enzymes, dynamic labeling experiments with ^{13}C-labeled methanol were performed. Throughout this study, several methanol/alcohol dehydrogenases as well as Hps Phi enzymes were tested for their activity (Tables 1 and 2). Because the Hps and Phi enzymes of *B. methanolicus* consistently performed best both in *in vivo* and *in vitro* assays (see above Table 2), they were selected for the ^{13}C labeling experiments using LC–MS. However, because Mdh examination resulted in conflicting results especially with respect to the effect of the activator protein Act (see Table 1), we tested the Mdh candidates more broadly with this approach. In a first screening we analyzed the incorporation of ^{13}C into hexose 6-phosphates in Δ*frmA E. coli* cells, which represent ideal metabolites because they are the first intermediates following C_1 fixation but they also provide information on precursor regeneration because incorporation of more than one atom of ^{13}C into hexose 6- phosphates can only be obtained *via* recycling of the acceptor carbon unit (Fig. 1). To analyze the performance of the different methanol oxidizing enzymes, cells were pre-grown on ribose to increase Hps Phi activity (see above) and subsequently transferred into medium without any carbon source to allow for monitoring of ribulose-5-phosphate regeneration. The experiments were started by addition of ^{13}C-labeled methanol, and label incorporation was followed over time. As selection parameters we determined first order time constants (T_{50}) for incor- poration of ^{13}C into hexose 6-phosphates and the maximally achieved labeling fraction in this metabolite dependent on the presence of the tested enzymes after ten minutes. Inspection of the collected data revealed that most of the different enzymes were inefficient and allowed almost no carbon incorporation from methanol into hexose 6-phosphates (Table 3). For these enzymes no detailed analysis was possible. Effective incorporation of carbon from methanol was only found for Mdh2 of *B. methanolicus* MGA3 and Mdh2 of *B. methanolicus* PB1. Mdh2 from *B. methanolicus* PB1 turned out to be slightly more efficient both in speed of label incorporation and maximal detectable labeling compared to the MGA3 enzyme (Table 3). This is in contrast to the results from previous experiments where Mdh2 of *B. methanolicus* MGA3 was the best performing enzyme *in vivo* based on formaldehyde

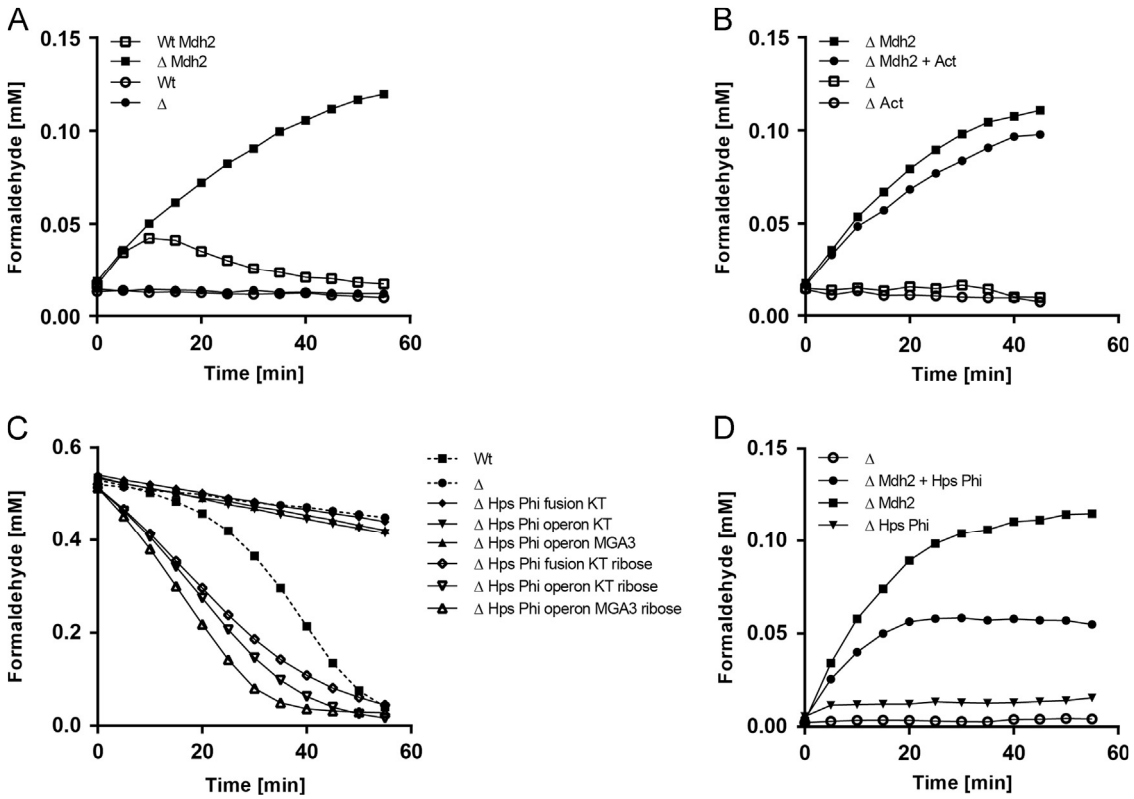

Fig. 2. *In vivo* formaldehyde assays. (A) Formaldehyde production *in vivo* in wild-type (open symbols) or Δ*frmA* (solid symbols) cells producing Mdh2 or carrying an empty plasmid. (B) Formaldehyde production in Δ*frmA* cells producing Mdh2 alone (squares) or Mdh2 and Act (circles) with the respective controls (open symbols).
(C) Formaldehyde degradation in Δ*frmA* cells in the presence (open symbols) or absence (closed symbols) of ribose for different Hps Phi constructs is shown. As a control, formaldehyde degradation in wild-type (squares, broken line) and Δ*frmA* (circles, broken line) cells not producing any enzymes is shown additionally. (D) Formaldehyde production of Δ*frmA* cells producing Mdh2, Hps and Phi. Cells not producing any enzyme (open circles), only Hps and Phi (upside down triangles) or only Mdh2 (squares), served as controls. If not indicated otherwise all enzymes used originate from *B. methanolicus* MGA3. Δ stands for Δ*frmA E. coli* cells. Mdhs are encoded on pSEVA424, Hps, Phi and Act are encoded on pSEVA131.

detection. Because we considered the ^{13}C labeling experiments to better reflect the *in vivo* condition, we used Mdh2 of *B. methanolicus* PB1 for further experiments. Interestingly, the presence of Act had neither a beneficial nor a negative effect on the activity of the tested enzymes. However, because its activating function has been consis- tently documented *in vitro* (Krog et al., 2013; Ochsner et al., 2014), we included Act in subsequent experiments.

Thus far the genes for the methanol oxidizing enzymes (Mdh, Adh), Hps, Phi and Act were all expressed from individual plasmids (see Supplementary Table 2). To simplify expression, *act* was either combined on one plasmid together with *mdh2* of *B. methanolicus* PB1 or on one plasmid together with *hps* and *phi*. Both versions were compared to cells producing all enzymes from three instead of two different plasmids. The maximal measured labeling and estimated time constant T_{50} were significantly lower when *mdh2* and *act* were expressed from the same plasmid (15.4% and 76.873.5 s), and the results with a strain encoding Hps, Phi and Act on the one plasmid were comparable especially with respect to the maximal level of detectable labeling (24% and 8473 s).

As mentioned above, *in silico* simulations and experimental data both showed that the endogenous formaldehyde detoxification path- way of *E. coli* is not essential for the conversion of methanol (Fig. 1), and in contrast it might actually be counterproductive by degrading formaldehyde produced by methanol oxidation (Fig. 2A). Nonetheless, we examined the effect of this pathway on the incorporation of carbon from methanol into biomass when all three essential enzymes were synthesized. To this end, we tested label incorporation efficiency based on % total labeling and the velocity of incorporation (T_{50}) in wild-type *E. coli* cells expressing *mdh2* of *B. methanolicus* PB1 from one plasmid and *hps, phi* and *act* from a second. Surprisingly, the maximal detectable labeling in these cells was within approximately 40% of the highest of all strains tested in this study (Table 2). To verify these findings, the experiment was repeated and the mean maximal labeling and the mean time constant for hexose 6-phospate of 5 independent biological replicates was determined. The maximal labeling detectable was highly reproducible and determined to be 38.272.8%. The mean time constant was more variable at 1447 28.6 s (Fig. 3A). Closer inspection of the mass isotopolog distribution in hexose 6-phosphates revealed that although 100% labeling was not achieved, a fraction of fully labeled metabolite was present (Fig. 4). This labeling result indicated that introducing Mdh, Hps and Phi established methanol assimilation in *E. coli*, and because up to 6 labeled carbons are found in hexose 6-phosphates, these molecules can pass several times through the entire RuMP cycle. This was further supported by the finding that label accumulation is also detectable in other metabolites of the RuMP cycle, *e.g.*, ribose 5- phosphate and ribulose 5-phosphate (Fig. 3B). In addition, labeling was detected in intermediates of lower glycolysis, *e.g.*, dihydroxyace- tone phosphate (DHAP) and phosphoenolpyruvate (Fig. 3B), which is assumed to operate in RuMP-cycle methylotrophs (Heggeset et al., 2012; Müller et al., 2014). Exemplarily we also analyzed labeling incorporation into UDP-N-acetylmuramic acid (UDP-MurNAc) and UDP-N-acetylglucosamine (UDP-GlcNac) which are precursors for cell wall biosynthesis and thus contribute to biomass formation. Significant labeling of 5.470.6% and 4.770.6%, respectively was detected in these molecules (Supplementary Table 3) showing that carbon molecules originating from methanol are not only used in central metabolism but appear in biosynthetic pathways as well.

Table 3
In vivo labeling results of engineered *E. coli* strains. Label incorporation into hexose 6-phosphates after addition of ^{13}C methanol is analyzed. None: first order fit of data not possible.

Enzyme combination	Max. labeling measured [%]	Max. labeling fit [%]	T_{50} [s]
Genetic background: Δ*frmA*			
Mdh2 *B. methanolicus* MGA3, Hps Phi, Act	20.2	20.270.6	68.270.5
Adh *D. kuznetsovii*, Hps Phi	0.2	None	None
Adh *D. kuznetsovii*, Hps Phi, Act	0.2	None	None
Adh *L. fusiformis*, Hps Phi	0.2	None	None
Adh *L. fusiformis*, Hps Phi, Act	3.7	None	None
Adh *B. coagulans*, Hps Phi	1.4	None	None
Adh *B. coagulans*, Hps Phi, Act	0.8	None	None
Adh *L. sphaericus*, Hps Phi	0	None	None
Adh *L. sphaericus*, Hps Phi, Act	0.4	None	None
Adh *D. hafniense*, Hps Phi	0.6	None	None
Adh *D. hafniense*, Hps Phi, Act	0.4	None	None
Mdh *B. methanolicus* PB1, Hps Phi	0.1	None	None
Mdh *B. methanolicus* PB1, Hps Phi, Act	0	None	None
Mdh2 *B. methanolicus* PB1, Hps Phi	26.3	25.772.5	63.772.3
Mdh2 *B. methanolicus* PB1, Hps Phi, Act	25.2	23.975	58.874.2
Mdh *B. methanolicus* MGA3 "NADP sensitive mutants", Hps Phi	0	None	None
Mdh *B. methanolicus* MGA3 "NADP sensitive mutants", Hps Phi, Act	0	None	None
Mdh2 *B. methanolicus* MGA3 "NADP sensitive mutants", Hps Phi	3.2	6.87285.8	681.2728.6
Mdh2 *B. methanolicus* MGA3 "NADP sensitive mutants", Hps Phi, Act	3.2	3.2719.3	128.672.1
Mdh *B. methanolicus* S97G, Hps Phi	0.05	None	None
Mdh *B. methanolicus* S97G, Hps Phi, Act	0	None	None
Mdh2 *B. methanolicus* S97G, Hps Phi	0	None	None
Mdh2 *B. methanolicus* S97G, Hps Phi, Act	0	None	None
Genetic background: wt			
Mdh2 *B. methanolicus* PB1, Hps, Phi, Act	39.4	4073.1	117.874.3

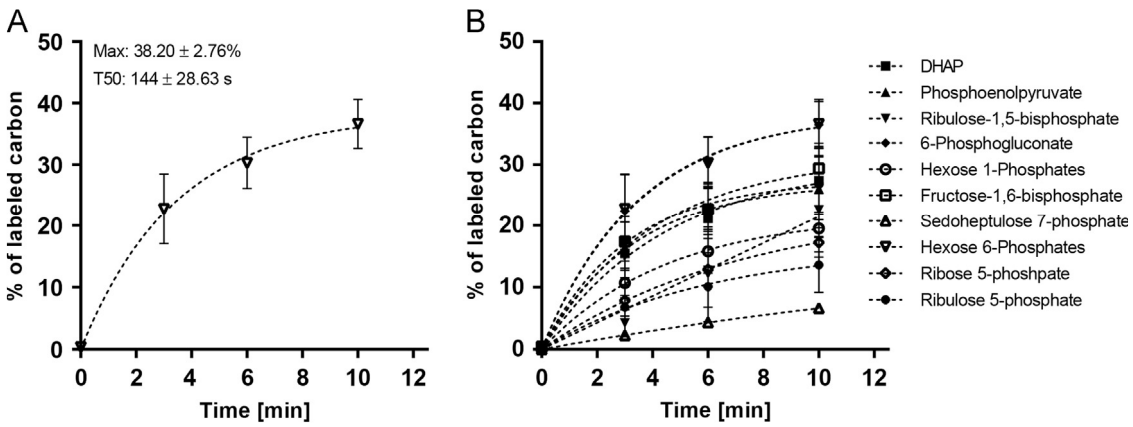

Fig. 3. ^{13}C-Label incorporation in wild-type *E. coli* cells from ^{13}C-methanol. ^{13}C-Label incorporation into hexose 6-phosphates (A) and other selected metabolites (B) in wild- type *E. coli* cells producing Mdh2 of *B. methanolicus* PB1, Hps, Phi and Act. Shown are the mean values of five biological replicates. Error bars indicate standard deviations and broken lines show first order fits. Results of fits are shown in Supplementary Table 3.

5. Discussion

In silico modeling suggested that introducing NAD-dependent Mdh and establishing the RuMP cycle for biomass formation represents a suitable strategy to enable *E. coli* to convert methanol into biomass. Additionally, practical considerations, taking into account the number of enzymes for gene transfer and the difficulty of producing highly complex proteins (*i.e.*, PQQ-dependent Mdh), made this solution most attractive. In total, heterologous production of three enzymes, Mdh, Hps, and Phi was predicted to be sufficient to allow biomass formation from methanol. To achieve the best possible results, several candidates for each enzyme were selected and tested in this study. For methanol oxidation *in vitro* we found that Mdh2 in the presence of the activator protein Act of *B. methanolicus* MGA3 was the most efficient. During *in vivo* tests based on the detection of formaldehyde production, this enzyme still performed best but the presence of Act had no positive effect on its activity. This finding was later confirmed during *in vivo* labeling experiments and raises the question whether the Act protein is indeed required *in vivo*. Notably, this query also holds for the donor organism *B. methanolicus*, where no *in vivo* function has yet been proven due to the failure to generate targeted knockouts. In this context, our finding is of interest that Mdh2 turned out to be of higher performance *in vivo* than Mdh, which is thought to represent the major enzyme for methanol oxidation in *B. methanolicus* (Brautaset et al., 2004) – again showing the need to develop a mutagenesis system for the natural host.

In vitro and *in vivo* testing of different Hps and Phi proteins showed the suitability of the respective enzymes also from *B. methanolicus* for active production in *E. coli*. Although the *in vitro* activities of these enzymes were high, their *in vivo* activities based on formaldehyde consumption were considerably lower. Further testing revealed that their activity increased if ribose was present during the experiments, pointing towards rapid depletion of the pentose phosphates, which are needed for fixation of formaldehyde.

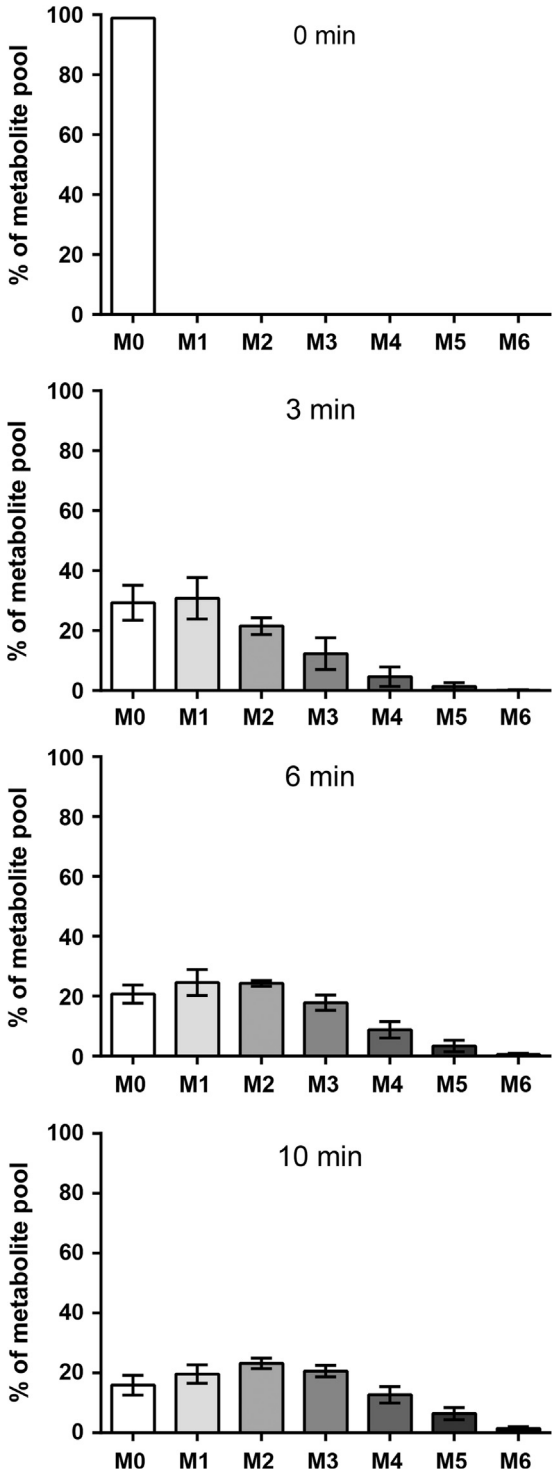

Fig. 4. Mass isotopolog distribution of hexose 6-phosphates. Distribution of mass isotopologs at different time points is shown for wild-type *E. coli* cells producing Mdh2 of *B. methanolicus* PB1, Hps, Phi and Act. The results of five biological replicates are shown. Error bars indicate standard deviations.

Comparison of *in vivo* formaldehyde production upon addition of methanol to cells producing only Mdh2 versus Mdh2, Hps and Phi revealed that formaldehyde produced by Mdh can be effi- ciently degraded by Hps and Phi. To analyze methanol conversion in more detail, we performed dynamic ^{13}C label incorporation experiments using LC-MS and analyzed methanol incorporation into metabolites over time. Emphasis was put on screening different Mdh derivatives because the *in vivo* results based on

formaldehyde accumulation revealed no increase in methanol utilization in the presence of Act. Testing all Mdh enzymes led to the finding that Mdh2 of *B. methanolicus* PB1 exhibits superior activity compared to Mdh2 of *B. methanolicus* MGA3. A maximal ^{13}C carbon labeling fraction of 40% was achieved for the wild-type strain producing Mdh2 together with Hps, Phi and Act combined on the same plasmid. Surprisingly, the *E. coli* wild-type background and not the Δ*frmA* background displayed the highest label incorporation. Although 100% labeling was thus not achieved, molecules containing 6 labeled carbons could be detected in hexose 6-phosphates. The latter are central metabolites both in endogenous *E. coli* pathways and in the newly established RuMP cycle. Incorporation of more than one labeled carbon (multiple- carbon-labeled hexose 6-phosphate species) can exclusively be explained by metabolites passing through the RuMP cycle several times, and it shows that the RuMP cycle is functional. The results achieved here represent a major step by introducing a novel pathway for C_1 utilization into *E. coli*. The major challenge in this approach seems to be the cyclic mode of operation of this pathway for biomass production which needs to operate in conjunction with the host's endogenous central metabolism to allow C_1 assimilation into biomass and growth in the presence of methanol as a sole carbon and energy source. Further improvement of the RuMP cycle by more balanced production of the utilized enzymes or even by exchanging them with enzymes from natural methylo- trophs such as *B. methanolicus* might represent a valuable strategy for overcoming potential problems caused by insufficient regen- eration of ribulose 5-phosphate as a precursor. Another potentially promising approach to increasing efficiency to allow *E. coli* to grow on methanol would be experimental evolution. Such appr- oaches have been applied successfully if basal activity of the enzymes or pathways could be established (Lee and Palsson, 2010). To this end, it might be advantageous to integrate the genes for the respective enzymes into the genome to allow more stable expression, especially over several generations. Even with- out increased efficiency, the strain generated in this study is able to convert methanol into central metabolites and holds the potential to convert methanol into value-added products if respective pathways are also introduced.

Acknowledgments

This study was supported by EU-FP7 Project PROMYSE "Products from Methanol by Synthetic Cell Factories" and by the European Science Foundation (ESF) 09-EuroSYNBIO-FP-023 SynMet Project, funded in part by SNF 31SY30-131039. We thank A. Ochsner and C. Mora (ETH Zurich) for support during determination of enzyme activities, P. Christen (ETH Zurich) for LC–MS support and L. Cottret (INSA Toulouse) for his help with *in silico* modeling. pSEVA plasmids were generously provided by V. De Lorenzo (CNB, Madrid).

References

Anthony, C., 1982. The Biochemistry of Methylotrophs. Academic Press, London; New York.

Anthony, C., 2004. The quinoprotein dehydrogenases for methanol and glucose. Arch. Biochem. Biophys. 428, 2–9.

Anthony, C., Williams, P., 2003. The structure and mechanism of methanol dehydrogenase. Biochim. Biophys. Acta 1647, 18–23.

Arfman, N., Bystrykh, L., Govorukhina, N.I., Dijkhuizen, L., 1990. 3-Hexulose-6- phosphate synthase from thermotolerant methylotroph *Bacillus* C1. Methods Enzymol. 188, 391–397.

Arfman, N., Hektor, H.J., Bystrykh, L.V., Govorukhina, N.I., Dijkhuizen, L., Frank, J., 1997. Properties of an NAD(H)-containing methanol dehydrogenase and its activator protein from *Bacillus methanolicus*. Eur. J. Biochem. 244, 426–433.

Arfman, N., Van Beeumen, J., De Vries, G.E., Harder, W., Dijkhuizen, L., 1991. Purification and characterization of an activator protein for methanol dehy- drogenase from thermotolerant *Bacillus* spp. J. Biol. Chem. 266, 3955–3960.

Arfman, N., Watling, E.M., Clement, W., van Oosterwijk, R.J., de Vries, G.E., Harder, W., Attwood, M.M., Dijkhuizen, L., 1989. Methanol metabolism in thermoto- lerant methylotrophic *Bacillus* strains involving a novel catabolic NAD- dependent methanol dehydrogenase as a key enzyme. Arch. Microbiol. 152, 280–288.

Brautaset, T., Jakobsen, M.O., Flickinger, M.C., Valla, S., Ellingsen, T.E., 2004. Plasmid- dependent methylotrophy in thermotolerant *Bacillus methanolicus*. J. Bacteriol. 186, 1229–1238.

Brautaset, T., Jakobsen, M.O., Joesefsen, K.D., Flickinger, M.C., Ellingsn, T.E., 2007. Bacillus methanolicus: a candidate for industrial production of mino acids from methanol at 50 degrees C. Appl. Microbia. Biotechnol. 74 (1), 22–34.

Case, G.L., Benevenga, N.J., 1977. Significance of formate as an intermediate in the oxidation of the methionine, S-methyl-L-cysteine and sarcosine methyl carbons to CO_2 in the rat. The Journal of nutrition 107, 1665–1676.

Chistoserdova, L., 2011. Modularity of methylotrophy, revisited. Environ. Microbiol. 13, 2603–2622.

Chistoserdova, L., Chen, S.W., Lapidus, A., Lidstrom, M.E., 2003. Methylotrophy in methylobacterium extorquens AM1 from a genomic point of view. J. Bacteriol. 185, 2980–2987.

Chistoserdova, L., Kalyuzhnaya, M.G., Lidstrom, M.E., 2009. The expanding world of methylotrophic metabolism. Annu. Rev. Microbiol. 63, 477–499.

Chistoserdova, L., Lapidus, A., Han, C., Goodwin, L., Saunders, L., Brettin, T., Tapia, R., Gilna, P., Lucas, S., Richardson, P.M., Lidstrom, M.E., 2007. Genome of *Methylo- bacillus flagellatus*, molecular basis for obligate methylotrophy, and polyphyletic origin of methylotrophy. J. Bacteriol. 189, 4020–4027.

Chistoserdova, L., Lidstrom, M.E., 2013. Aerobic methylotrophic prokaryotes, The prokaryotes. Springer, Berlin, Heidelberg, pp. 267–285.

Cormack, B., Castano, I., 2002. Introduction of point mutations into cloned genes. Methods Enzymol. 350, 199–218.

Duine, J.A., 1999. Thiols in formaldehyde dissimilation and detoxification. Biofactors 10, 201–206.

Erb, T.J., Berg, I.A., Brecht, V., Müller, M., Fuchs, G., Alber, B.E., 2007. Synthesis of C5-dicarboxylic acids from C2-units involving crotonyl-CoA carboxylase/reduc- tase: the ethylmalonyl-CoA pathway. Proc. Natl. Acad. Sci. USA 104, 10631–10636.

Feist, A.M., Henry, C.S., Reed, J.L., Krummenacker, M., Joyce, A.R., Karp, P.D., Broadbelt, L.J., Hatzimanikatis, V., Palsson, B.O., 2007. A genome-scale meta- bolic reconstruction for *Escherichia coli* K-12 MG1655 that accounts for 1260 ORFs and thermodynamic information. Mol. Syst. Biol. 3, 121.

Fischer, E., Zamboni, N., Sauer, U., 2004. High-throughput metabolic flux analysis based on gas chromatography-mass spectrometry derived 13C constraints. Anal. Biochem. 325, 308–316.

Goenrich, M., Bartoschek, S., Hagemeier, C.H., Griesinger, C., Vorholt, J.A., 2002. A glutathione-dependent formaldehyde-activating enzyme (Gfa) from *Para- coccus denitrificans* deteced and purified via two-dimensonal proton exchange NMR spectroscopy. J. Biol. Chem. 277, 3069–3072.

Gonzalez, C.F., Proudfoot, M., Brown, G., Korniyenko, Y., Mori, H., Savchenko, A.V., Yakunin, A.F., 2006. Molecular basis of formaldehyde detoxification. Character- ization of two S-formylglutathione hydrolases from *Escherichia coli*, FrmB and YeiG. J. Biol. Chem. 281, 14514–14522.

Green, M.R., Sambrook, J., Sambrook, J., 2012. Molecular Cloning: A Laboratory Manual. Cold Spring Harbor Laboratory Press, Cold Spring Harbor, NY.

Gutheil, W.G., Holmquist, B., Vallee, B.L., 1992. Purification, characterization, and partial sequence of the glutathione-dependent formaldehyde dehydrogenase from *Escherichia coli*: a class III alcohol dehydrogenase. Biochemistry 31, 475–481.

Heggeset, T.M., Krog, A., Balzer, S., Wentzel, A., Ellingsen, T.E., Brautaset, T., 2012. Genome sequence of thermotolerant *Bacillus methanolicus*: features and reg- ulation related to methylotrophy and production of L-lysine and L-glutamate from methanol. Appl. Environ. Microbiol. 78, 5170–5181.

Hektor, H.J., Kloosterman, H., Dijkhuizen, L., 2002. Identification of a magnesium- dependent NAD(P)(H)-binding domain in the nicotinoprotein methanol dehy- drogenase from *Bacillus methanolicus*. J. Biol. Chem. 277, 46966–46973.

Irla, M., Neshat, A., Winkler, A., Albersmeier, A., Heggeset, T.M., Brautaset, T., Kalinowski, J., Wendisch, V.F., Ruckert, C., 2014. Complete genome sequence of *Bacillus methanolicus* MGA3, a thermotolerant amino acid producing methylo- troph. J. Biotechnol. 188C, 110–111.

Kallen, R.G., Jencks, W.P., 1966a. The dissociation constants of tetrahydrofolic acid. J. Biol. Chem. 241, 5845–5850.

Kallen, R.G., Jencks, W.P., 1966b. The mechanism of the condensation of formalde- hyde with tetrahydrofolic acid. J. Biol. Chem. 241, 5851–5863.

Kay, L.D., Osborn, M.J., Hatefi, Y., Huennekens, F.M., 1960. The enzymatic conversion of N5-formyl tetrahydrofolic acid (folinic acid) to N10-formyl tetrahydrofolic acid. J. Biol. Chem. 235, 195–201.

Kiefer, P., Delmotte, N., Vorholt, J.A., 2011. Nanoscale ion-pair reversed-phase HPLC–MS for sensitive metabolome analysis. Anal. Chem. 83, 850–855.

Kiefer, P., Schmitt, U., Vorholt, J.A., 2013. eMZed: an open source framework in Python for rapid and interactive development of LC/MS data analysis work- flows. Bioinformatics 29, 963–964.

Krog, A., Heggeset, T.M., Müller, J.E., Kupper, C.E., Schneider, O., Vorholt, J.A., Ellingsen, T.E., Brautaset, T., 2013. Methylotrophic *Bacillus methanolicus* encodes two chromosomal and one plasmid born NAD(þ)-dependent methanol dehy- drogenase paralogs with different catalytic and biochemical properties. PLoS One 8, e59188.

Kung, Y., Runguphan, W., Keasling, J.D., 2012. From fields to fuels: recent advances in the microbial production of biofuels. ACS Synth. Biol. 1, 498–513.

Lee, D.H., Palsson, B.O., 2010. Adaptive evolution of *Escherichia coli* K-12 MG1655 during growth on a Nonnative carbon source, L-1,2-propanediol. Appl. Environ. Microbiol. 76, 4158–4168.

Maclenna, Dg, Gow, J.S., Stringer, D.A., 1973. Methanol-bacterium process for Scp. Process Biochem. 8, 22–24.

Marx, C.J., Bringel, F., Chistoserdova, L., Moulin, L., Farhan Ul Haque, M., Fleischman, D.E., Gruffaz, C., Jourand, P., Knief, C., Lee, M.C., Muller, E.E., Nadalig, T., Peyraud, R., Roselli, S., Russ, L., Goodwin, L.A., Ivanova, N., Kyrpides, N., Lajus, A., Land, M.L., Medigue, C., Mikhailova, N., Nolan, M., Woyke, T., Stolyar, S., Vorholt, J.A., Vuilleumier, S., 2012. Complete genome sequences of six strains of the genus *Methylobacterium*. J. Bacteriol. 194, 4746–4748.

Mattozzi, M., Ziesack, M., Voges, M.J., Silver, P.A., Way, J.C., 2013. Expression of the sub-pathways of the *Chloroflexus aurantiacus* 3-hydroxypropionate carbon fixation bicycle in *E. coli*: toward horizontal transfer of autotrophic growth. Metab. Eng. 16, 130–139.

Müller, J.E., Litsanov, B., Bortfeld-Miller, M., Trachsel, C., Grossmann, J., Brautaset, T., Vorholt, J.A., 2014. Proteomic analysis of the thermophilic methylotroph *Bacillus methanolicus* MGA3. Proteomics 14, 725–737.

Nash, T., 1953. The colorimetric estimation of formaldehyde by means of the Hantzsch reaction. Biochem. J. 55, 416–421.

Nicolas, C., Kiefer, P., Letisse, F., Kromer, J., Massou, S., Soucaille, P., Wittmann, C., Lindley, N.D., Portais, J.C., 2007. Response of the central metabolism of *Escherichia coli* to modified expression of the gene encoding the glucose-6- phosphate dehydrogenase. FEBS Lett. 581, 3771–3776.

Ochsner, A.M., Müller, J.E., Mora, C.A., Vorholt, J.A., 2014. *In vitro* activation of NAD- dependent alcohol dehydrogenases by Nudix hydrolases is more widespread than assumed. FEBS Lett.

Olah, G.A., 2013. Towards oil independence through renewable methanol chem- istry. Angew. Chem. 52, 104–107.

Orita, I., Sakamoto, N., Kato, N., Yurimoto, H., Sakai, Y., 2007. Bifunctional enzyme fusion of 3-hexulose-6-phosphate synthase and 6-phospho-3-hexuloisomerase. Appl. Microbiol. Biotechnol. 76, 439–445.

Orita, I., Yurimoto, H., Hirai, R., Kawarabayasi, Y., Sakai, Y., Kato, N., 2005. The archaeon *Pyrococcus horikoshii* possesses a bifunctional enzyme for formaldehyde fixation via the ribulose monophosphate pathway. J. Bacteriol. 187, 3636–3642.

Peyraud, R., Kiefer, P., Christen, P., Massou, S., Portais, J.C., Vorholt, J.A., 2009. Demonstration of the ethylmalonyl-CoA pathway by using C-13 metabolomics. Proc. Natl. Acad. Sci. USA 106, 4846–4851.

Quayle, J.R., 1982. 3-Hexulose-6-phosphate synthase from *Methylomonas* (*Methy- lococcus*) *capsulatus*. Methods Enzymol. 90 (Pt E), 314–319.

Ro, D.K., Ouellet, M., Paradise, E.M., Burd, H., Eng, D., Paddon, C.J., Newman, J.D., Keasling, J.D., 2008. Induction of multiple pleiotropic drug resistance genes in yeast engineered to produce an increased level of anti-malarial drug precursor, artemisinic acid. BMC Biotechnol. 8, 83.

Rocha, I., Maia, P., Evangelista, P., Vilaca, P., Soares, S., Pinto, J.P., Nielsen, J., Patil, K.R., Ferreira, E.C., Rocha, M., 2010. OptFlux: an open-source software platform for in silico metabolic engineering. BMC Syst. Biol. 4, 45.

Schrader, J., Schilling, M., Holtmann, D., Sell, D., Filho, M.V., Marx, A., Vorholt, J.A., 2009. Methanol-based industrial biotechnology: current status and future perspectives of methylotrophic bacteria. Trends Biotechnol. 27, 107–115.

Shih, P.M., Zarzycki, J., Niyogi, K.K., Kerfeld, C.A., 2014. Introduction of a synthetic CO(2)-fixing photorespiratory bypass into a cyanobacterium. J. Biol. Chem. 289, 9493–9500.

Silva-Rocha, R., Martinez-Garcia, E., Calles, B., Chavarria, M., Arce-Rodriguez, A., de Las Heras, A., Paez-Espino, AD., Durante-Rodriguez, G., Kim, J., Nikel, P.I., Platero, R., de Lorenzo, V., 2013. The Standard European Vector Architecture (SEVA): a coherent platform for the analysis and deployment of complex prokaryotic phenotypes. Nucl. Acids Res. 41, D666–D675.

Solomons, G.L., 1983. Single cell protein. Crit. Rev. Biotechnol. 1, 21–58.

Vorholt, J.A., 2002. Cofactor-dependent pathways of formaldehyde oxidation in methylotrophic bacteria. Arch. Microbiol. 178, 239–249.

Vorholt, J.A., Marx, C.J., Lidstrom, M.E., Thauer, R.K., 2000. Novel formaldehyde- activating enzyme in *Methylobacterium extorquens* AM1 required for growth on methanol. J. Bacteriol. 182, 6645–6650.

Vuilleumier, S., Chistoserdova, L., Lee, M.C., Bringel, F., Lajus, A., Zhou, Y., Gourion, B., Barbe, V., Chang, J., Cruveiller, S., Dossat, C., Gillett, W., Gruffaz, C., Haugen, E., Hourcade, E., Levy, R., Mangenot, S., Müller, E., Nadalig, T., Pagni, M., Penny, C., Peyraud, R., Robinson, D.G., Roche, D., Rouy, Z., Saenampechek, C., Salvignol, G., Vallenet, D., Wu, Z., Marx, C.J., Vorholt, J.A., Olson, M.V., Kaul, R., Weissenbach, J., Medigue, C., Lidstrom, M.E., 2009. *Methylobacterium* genome sequences: a reference blueprint to investigate microbial metabolism of C1 compounds from natural and industrial sources. PLoS One 4, e5584.

Wagh, J., Shah, S., Bhandari, P., Archana, G., Kumar, G.N., 2014. Heterologous expression of pyrroloquinoline quinone (pqq) gene cluster confers mineral phosphate solubilization ability to Herbaspirillum seropedicae Z67. Appl. Microbiol. Biotechnol. 98, 5117–5129.

Ward, N., Larsen, O., Sakwa, J., Bruseth, L., Khouri, H., Durkin, A.S., Dimitrov, G., Jiang, L., Scanlan, D., Kang, K.H., Lewis, M., Nelson, K.E., Methe, B., Wu, M., Heidelberg, J.F., Paulsen, I.T., Fouts, D., Ravel, J., Tettelin, H., Ren, Q., Read, T., DeBoy, R.T., Seshadri, R., Salzberg, S.L., Jensen, H.B., Birkeland, N.K., Nelson, W. C., Dodson, R.J., Grindhaug, S.H., Holt, I., Eidhammer, I., Jonasen, I., Vanaken, S., Utterback, T., Feldblyum, T.V., Fraser, C.M., Lillehaug, J.R., Eisen, J.A., 2004. Genomic insights into methanotrophy: the complete genome sequence of *Methylococcus capsulatus* (Bath). PLoS Biol. 2, e303.

Way, J.C., Collins, J.J., Keasling, J.D., Silver, P.A., 2014. Integrating biological redesign: where synthetic biology came from and where it needs to go. Cell 157, 151–161.

Westlake, R., 1986. Large-scale continuous production of single cell protein. Chem. Ing. Tech. 58, 934–937.

Windass, J.D., Worsey, M.J., Pioli, E.M., Pioli, D., Barth, P.T., Atherton, K.T., Dart, E.C., Byrom, D., Powell, K., Senior, P.J., 1980. Improved conversion of methanol to single-cell protein by Methylophilus methylotrophus. Nature 287, 396–401.

Yang, X.P., Zhong, G.F., Lin, J.P., Mao, D.B., Wei, D.Z., 2010. Pyrroloquinoline quinone biosynthesis in *Escherichia coli* through expression of the *Gluconobacter oxydans* pqqABCDE gene cluster. J. Ind. Microbiol. Biotechnol. 37, 575–580.